RETRIEVAL ALGORITHMS FOR ATMOSPHERIC ATTENUATION IN THE FREQUENCY BAND 15 – 52 GHz FROM TWO-CHANNEL MICROWAVE RADIOMETER OBSERVATIONS

Peter Forkman, Patrick Eriksson, and Gunnar Elgered

Department of Space, Earth and Environment, Chalmers University of Technology, Gothenburg, Sweden

Abstract

Retrieval algorithms for atmospheric transmission, signal propagation path delay, atmospheric water vapour and liquid water contents have been produced within the context of a prototype development of a dual-channel microwave radiometer. The errors found match what is achieved by existing radiometers. The requirement formulated by ESA for the transmission retrieval is met. In fact, this requirement is met with some margin allowing for additional offset errors in the atmospheric attenuation coefficients and in the two radiometer channels which have not been included in the simulations.

Key words: atmospheric transmission, microwave radiometry, signal delay, water vapour, liquid water.

1. INTRODUCTION

Ground-based microwave radiometers operating in the frequency range 20–40 GHz have several applications using atmospheric remote sensing techniques. Often the basic idea is to measure the atmospheric sky brightness temperature on and off the water vapour emission line centred just above 22 GHz. These temperatures may be used to infer atmospheric transmission (or absorption) [1] as well as the signal propagation path delay through the atmosphere in the direction of the observation [2][3]. Because the main atmospheric constituents determining the sky brightness temperatures are the integrated amounts of water vapour (IWV) and liquid water (ILW) also these quantities may be estimated [4], [5] and [6]. We will refer to this instrument as a water vapour radiometer (WVR).

In this study the focus is on the estimation of atmospheric transmission along earth-space paths although we also present example results for the other applications mentioned above. We have developed these algorithms for a site at the Onsala Space Observatory on the Swedish west coast. A prototype WVR, developed by Omnisys Instruments, Gothenburg, Sweden, for which the derived algorithms are intended is shown at the test site in Figure 1.

Here we first, in Section 2, describe the simulations of sky brightness temperatures and the approaches used in the modelling work needed to estimate the relevant parameters. The obtained results, in terms of the expected accuracy, are presented in Section 3. Finally, in Section 4, we give the conclusions of the study.

2. SIMULATIONS

2.1. Input data and assumptions

The input data describing the atmospheric properties were taken from ERA-Interim via its web interface [7]. The quantities used are: surface pressure, temperature profile, geopotential altitude, humidity profile, liquid water content profile (LWC) and low cloud fraction (LCF). Data were downloaded for the years 2000–2013, for 00, 06, 12 and 18 UT at the highest available resolution. The position was selected to match the location of the Onsala Space Observatory, OSO. This atmospheric database contained 20,456 cases.

Figure 1. The prototype WVR Orwvar installed for test measurements at the Onsala Space Observatory. Orwar is an acronym for "Omnisys radiometer for water vapour and atmospheric research". The GNSS station ONSA, part of the global International GNSS Service (IGS) network [8], is seen in the background to the left.

The following assumptions were made about the WVR:

1. the instrument has two channels, centred at 23.8 GHz and 31.4 GHz;
2. the antenna pattern is sufficiently narrow, that a pencil beam calculation represents the antenna temperature;
3. the instrument channels are sufficiently narrow that a monochromatic calculation represents the brightness temperature;
4. the magnitude of uncorrelated (thermal) noise is assumed to be 0.6 K, for both channels (including noise added by the atmosphere and the calibration process);
5. there are fully correlated errors between the two channels (0.37 K rms in channel 1 and 0.47 K rms in channel 2);
6. all instrument errors are assumed to be independent of the observed air mass.

The mentioned instrument errors are estimates and must be verified by actual measurements.

The observation database produced by the ARTS forward model [9] covers 15 GHz to 52 GHz, in steps of 200 MHz, and holds data for two different viewing angles matching air mass factors 1 and 2. In this specific study the following quantities were calculated: brightness temperature, transmission, wet propagation delay, integrated zenith water vapour, IWV, and integrated zenith liquid water (cloud water), ILW.

Comparison to existing observations at OSO revealed that the ERA-Interim data seem to underestimate both the occurrence frequency and maximum values of ILW. The liquid water data were modified according to the following scheme:

1. The LWC (at all altitudes) was set to 0 if ILW < 0.035 mm and LCF $< \ell$, where ℓ is a random number with a at distribution between 0 and 1. That is, the instrument was assumed to be in the cloud free portion of the model grid box as long as the ILW of the model is relatively low.
2. For ILW > 0.035 mm the instrument was always considered to be placed in the cloudy part of the grid box, and the LWC from ERA-Interim is increased with a factor of 3.

2.2. Regression model

Measured brightness temperatures are used to model the atmospheric properties by polynomial expressions. The polynomials applied are of second order (except for ILW) and include a cross-term:

$$t(\nu,\epsilon) = a_0(\nu,\epsilon) + a_1(\nu,\epsilon)\cdot r_1 + a_2(\nu,\epsilon)\cdot r_2 + a_3(\nu,\epsilon)\cdot r_1^2 + a_4(\nu,\epsilon)\cdot r_2^2 + a_5(\nu,\epsilon)\cdot r_1\cdot r_2 \quad (1)$$

where retrieval of the transmission, t at the frequency ν and the elevation angle ϵ is used as an example, and a_0, a_1 ... are the polynomial coefficients to be determined. The studied atmospheric properties are related to the transmission, therefore r_1 is chosen to be t for channel 1 and r_2 is t for channel 2. The one-layer model of the atmospheric radiative transfer, is given by:

$$T_b(\nu,\epsilon) = T_{bg}\, e^{-\tau(\nu,\epsilon)} + T_{eff}(\nu)\,\left(1 - e^{-\tau(\nu,\epsilon)}\right) \quad (2)$$

where $T_b(\nu,\epsilon)$ is the observed brightness temperature, T_{bg} is the cosmic background temperature, $e^{-\tau}$ is the atmospheric transmission, t, and T_{eff} is the effective temperature of the atmosphere. The parameter t, and hence r in this case, can be expressed as:

$$r(\nu,\epsilon) = t(\nu,\epsilon) = \left(\frac{T_{eff}(\nu) - T_b(\nu,\epsilon)}{T_{eff}(\nu) - T_{bg}}\right) \quad (3)$$

The effective temperature T_{eff} is often approximated with $T_{eff} = 0.95\cdot T_{gr}$, where T_{gr} is the temperature at the ground. We have used the ARTS database of t, T_b and T_{gr} to estimate refined T_{eff} approximations for the two WVR channels, see Table 1.

Table 1. The effective temperature T_{eff} at the frequencies of the WVR channels

Channel	Frequency [GHz]	T_{eff} [K]	1 σ [K]
1	23.8	0.959·T_{gr}	2.50
2	31.4	0.951·T_{gr}	3.47

For the ILW a higher order polynomial is applied:

$$\text{ILW} = a_0(\epsilon) + a_1(\epsilon)\cdot r_1 + a_2(\epsilon)\cdot r_2 + a_3(\epsilon)\cdot r_1^2 + a_4(\epsilon)\cdot r_2^2 + a_5(\epsilon)\cdot r_1 r_2 + a_6(\epsilon)\cdot r_1^3 + a_7(\epsilon)\cdot r_2^3 \quad (4)$$

As indicated in Equation 1, fitting variables must be derived for each frequency and elevation where the transmission shall be determined. For the retrieval of IWV, ILW, and zenith wet delay, ZWD, there is no frequency or elevation dependency. However, it is preferable to use T_b at a low elevation to get as good estimates as possible. The polynomial coefficients are affected by the chosen elevation angle of the observation.

The Onsala site is used for testing and demonstration of the retrieval performance, but the retrievals can easily be adopted to the conditions at other sites given that the atmospheric data used to determine the regression coefficients are taken from a global atmospheric model, such as the ERA-Interim. Selected output parameters both from the ERA-Interim dataset and from calculations by ARTS are illustrated in Figure 2. Note that the relation between ZWD and IWV is approximately linear [10]: ZWD [mm] = $Q\cdot$ IWV [kg/m^2], where Q varies from 6.1 to 6.9 when the effective temperature of the wet refractivity varies from 285 K to 250 K.

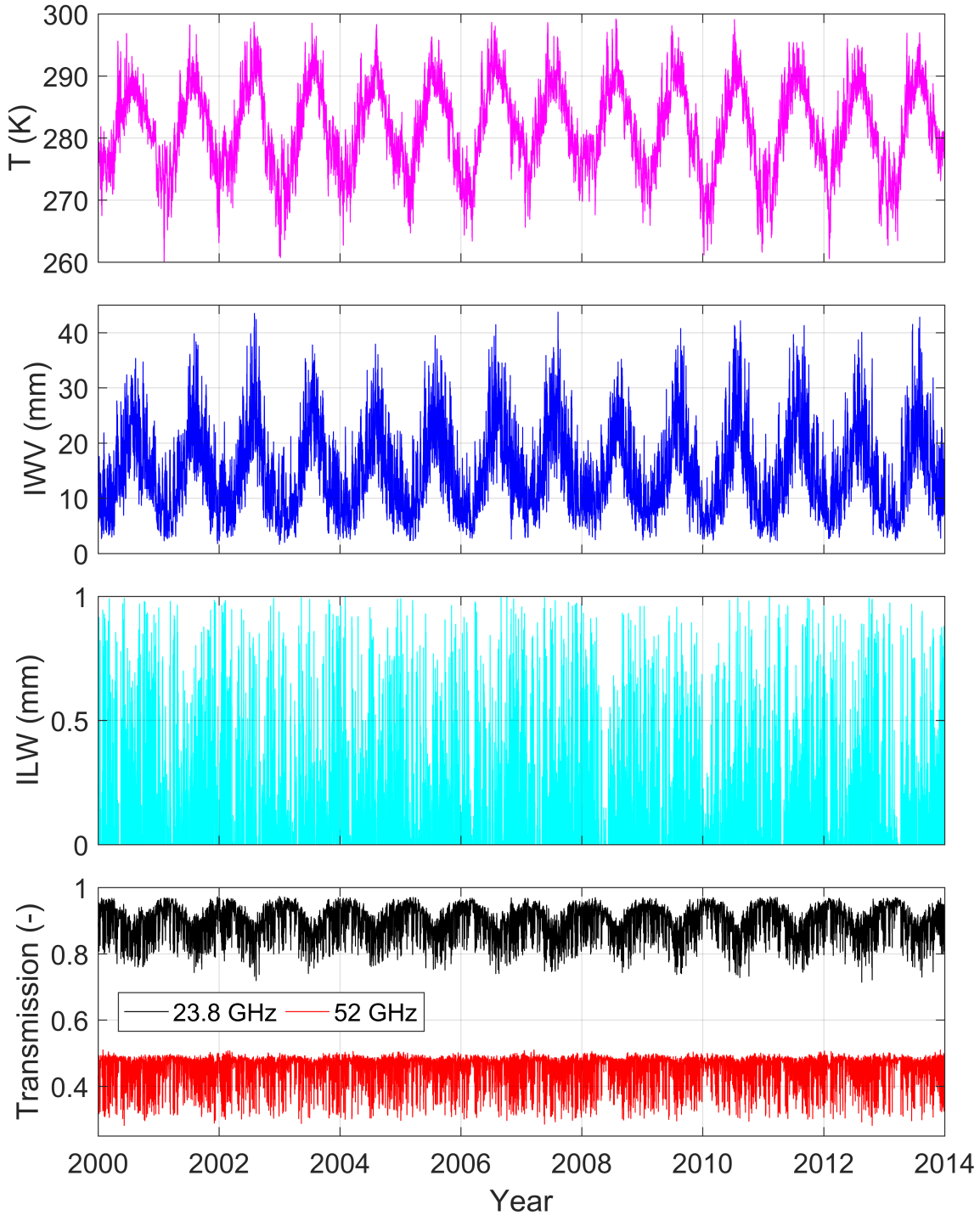

Figure 2. Output parameters from ERA-Interim and the ARTS forward model (from top to bottom): ground temperature, IWV, ILW and the transmission at 23.8 and 52.0 GHz for the studied time period. Only data when ILW $<$ 1 mm are included.

3. RESULTS

The regression model is derived using the database of simulated observations (without noise), and the errors are estimated by using the same data with noise added (both correlated and uncorrelated). For example, the matrix form $M \cdot a = x$, where x is a vector with the atmospheric parameters we like to study, can be written as:

$$\begin{pmatrix} 1 & r_{11} & r_{21} & r_{11}^2 & r_{21}^2 & r_{11}r_{21} \\ 1 & r_{12} & r_{22} & r_{12}^2 & r_{22}^2 & r_{12}r_{22} \\ \cdots & \cdots & \cdots & \cdots & \cdots & \cdots \\ 1 & r_{1n} & r_{2n} & r_{1n}^2 & r_{2n}^2 & r_{1n}r_{2n} \end{pmatrix} \cdot \begin{pmatrix} a_0 \\ a_1 \\ a_2 \\ a_3 \\ a_4 \\ a_5 \end{pmatrix} = \begin{pmatrix} x_1 \\ x_2 \\ \cdot\cdot \\ x_n \end{pmatrix} \tag{5}$$

where n is the number of used ERA-Interim profiles (19,820). When the polynomial coefficients, a_i are calculated the correlated and uncorrelated noise, N, are added to the r-factors (see Equation 3) to form the M_N matrix. Finally, the parameter x including noise is given by $x_N = M_N \cdot a$. Both correlated and uncorrelated noise are added to the T_b values for channel 1 and 2 as described in Section 2. Uncorrelated noise are added to the T_{eff} values as shown in Table 1.

We have removed the ERA-Interim profiles where ILW $>$ 1 mm since, based on our experience, it is a high probability for rain when the integrated liquid water exceeds 1 mm. This implied that about 3 % of the profiles were removed.

3.1. Atmospheric transmission

Figure 3 depicts the zenith transmissions for the ERA-Interim dataset calculated with ARTS. The 1 σ and the maximum total error are also shown. The steep gradient towards low transmissions above 45 GHz is explained by the band of oxygen lines in the frequency range 50–70 GHz.

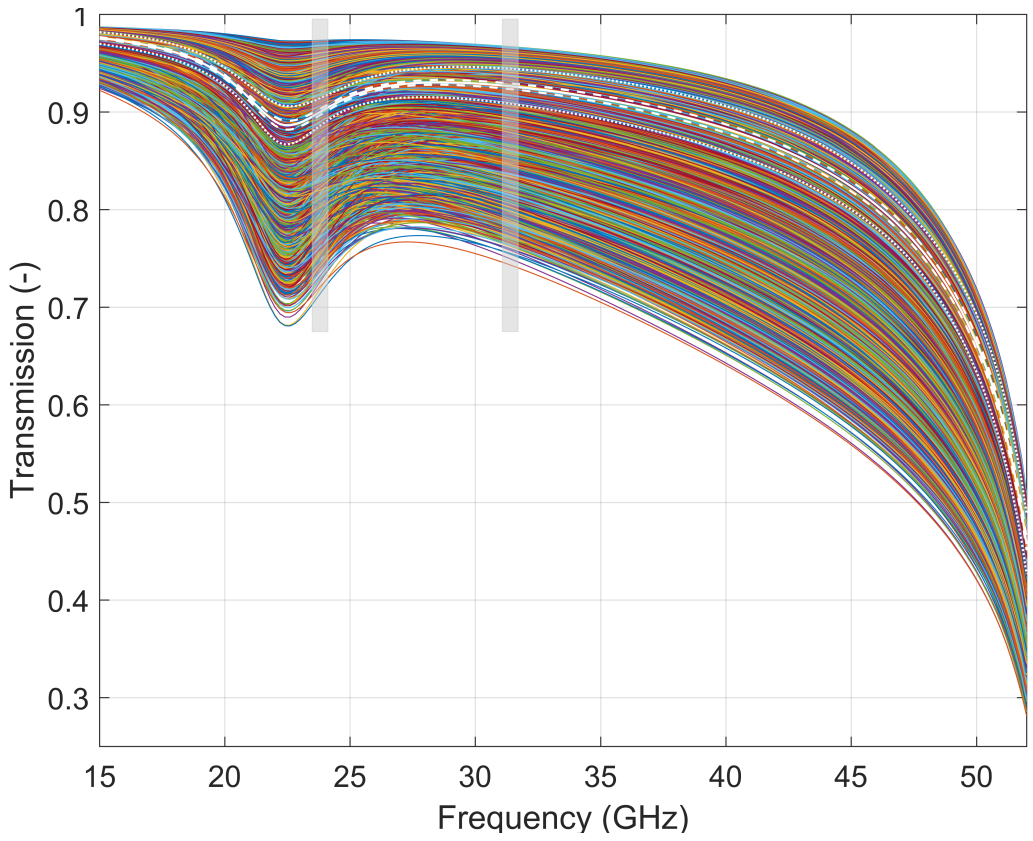

Figure 3. Transmissions at one air mass for the ERA-Interim profiles are shown for the cases when the ILW $<$ 1 mm. The solid white line shows the mean transmission; the dashed white lines show the $\pm 1\sigma$ total error; and the dotted white lines show the interval for the maximum total error. The vertical grey bars show the two observed frequency bands.

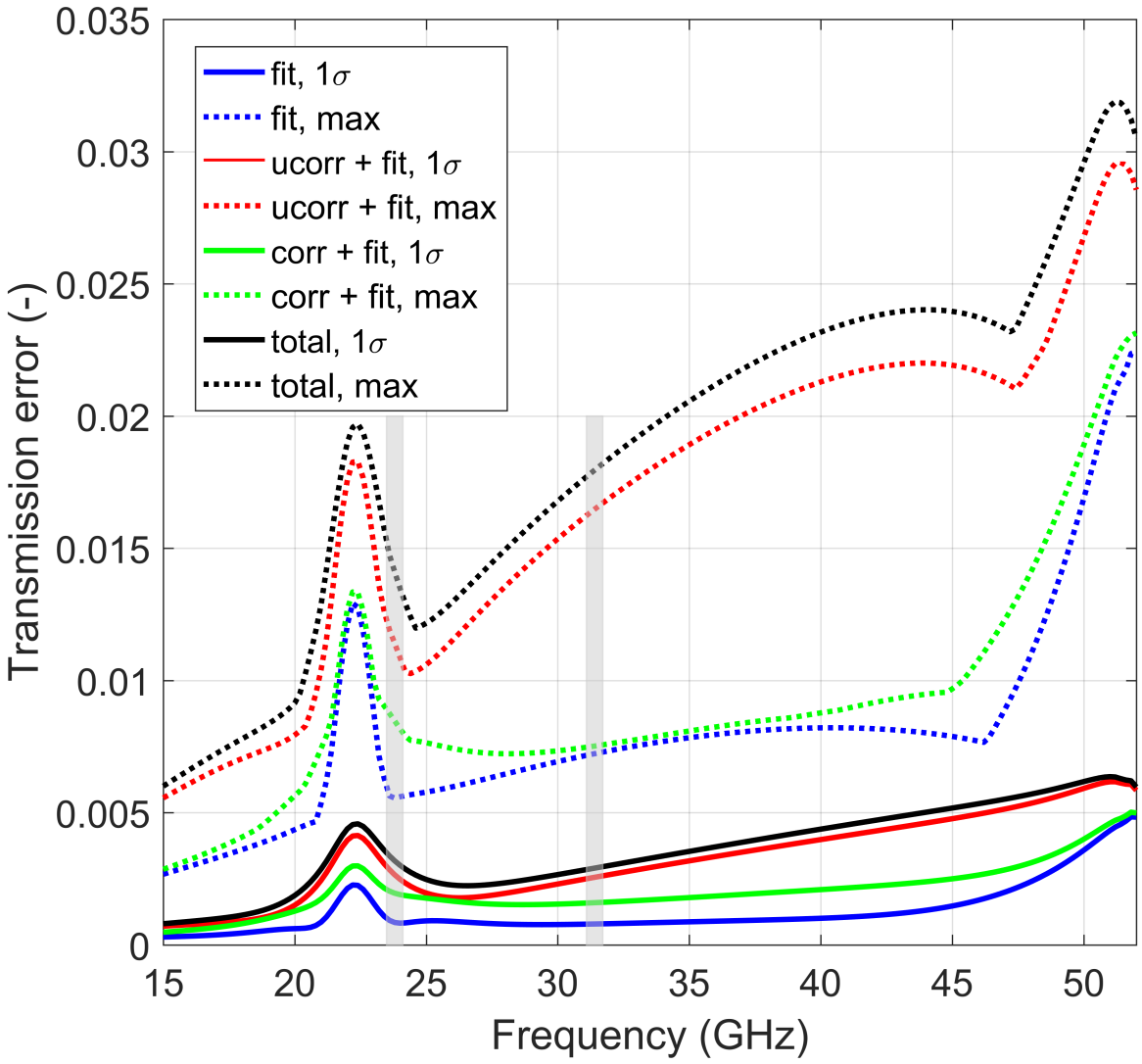

Figure 4. Transmission errors for the ERA-Interim profiles, where profiles having the ILW $<$ 1 mm are are included in the calculations. The vertical grey bars show the two observed frequency bands.

Using Equation 5, with observations at one air mass, we calculate the expected transmission error as a function of frequency.

Figure 4 includes several errors. The term ”fit error” (blue lines) refers to the error in absence of measurement uncertainties, i.e. those that originates solely from basic limitations of the measurement. Limitations of the regression fit would also end up as a fit error, but this contribution appears to be very small compared to the intrinsic smoothing error. (This conclusion is drawn from observing that more complex fit models do not decrease the fit error.) The ESA requirements for the accuracy of the inferred transmission is that that the 1-σ total error shall be $<$ 0.01, which is met with margins in the 15–52 GHz frequency range.

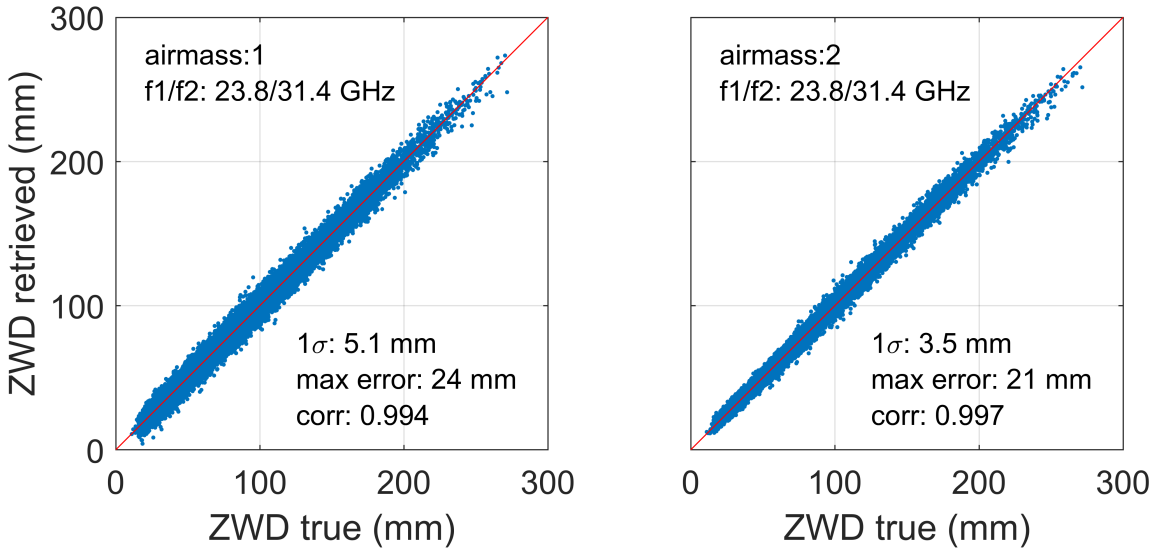

Figure 5. Retrieval of zenith wet delays, ZWD, where the zenith integrated liquid water < 1 mm. In the left plot observations at one air mass are used and in the right plot observations at two air masses are used.

3.2. Zenith wet delay (ZWD), integrated water vapour (IWV) and integrated liquid water (ILW)

In Figure 5 we present the retrieval of ZWD using observations of T_b at both one and two air masses. Observations at a high air mass (low elevation) gives higher brightness temperatures compared to observations at a low air mass. Since all errors are assumed to be independent of the observed air mass, the errors will have less relative importance when observing at two air masses instead of at one. This is clearly seen in Figure 5.

Figure 6 illustrates the retrieval of IWV and ILW. The observations are acquired at two air masses, but the IWV and ILW are referred to the zenith direction.

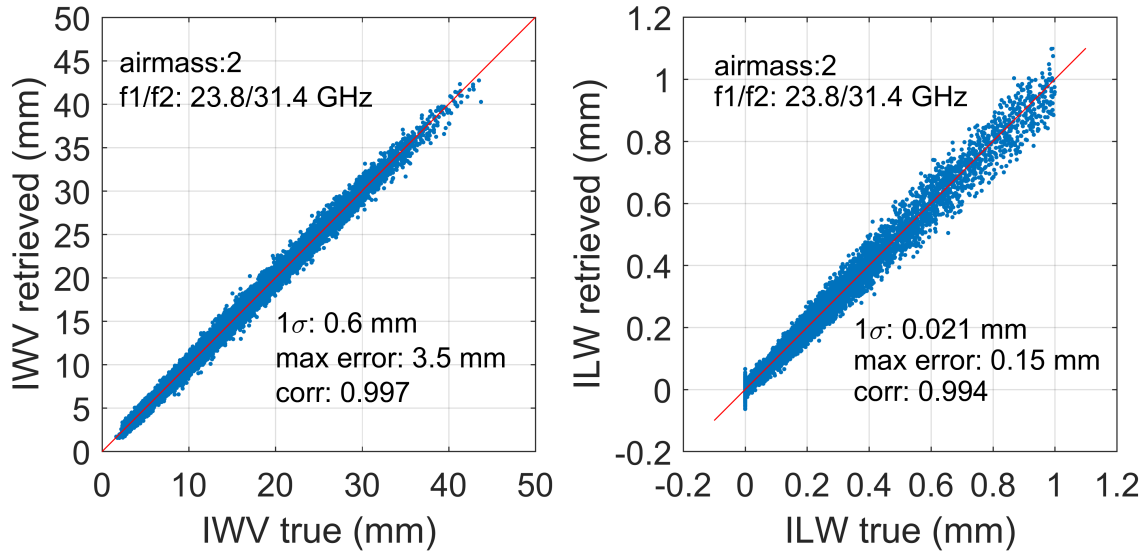

Figure 6. The left plot depicts retrieval of zenith integrated water vapour (IWV). The right plot depicts retrieval of zenith integrated liquid water (ILW). ILW < 1 mm and observations at two air masses are used.

4. CONCLUSIONS

A retrieval set-up based on the ARTS forward model and a polynomial regression model is presented. The OSO site is used for testing and demonstration of the retrieval performance, but the retrievals can easily be adopted to the conditions at other sites as the atmospheric data used to determine the regression coefficients are taken from a global atmospheric model (ERA-Interim). The errors found should be acceptable and match what is achieved by existing radiometers. The requirement specified for the transmission retrieval is met. In fact, the requirement is met with some margin implying that bias errors in the atmospheric attenuation coefficients (see e.g. [11]) and in the instrument, which have not been included in the simulations, can be tolerated to some extent.

REFERENCES

[1] Westwater, E.R., Snider, J.B. and Falls, M.J. (1990). Ground-based radiometric observations of atmospheric emission and attenuation at 20.6, 31.65, and 90 GHz: A comparison of measurements and theory, IEEE Trans. Antennas Propag., AP-38, pp. 1569–1580, https://doi.org/10.1109/8.59770.

[2] Elgered, G. (1993). Tropospheric Radio Path Delay from Ground-Based Microwave Radiometry, Atmospheric Remote Sensing by Microwave Radiometry, ed. M. Janssen, Wiley & Sons, pp. 215–258, New York.

[3] Klügel, T., Böer, A., Schüler, T., and Schwarz, W. (2019). Atmospheric data set from the Geodetic Observatory Wettzell during the CONT-17 VLBI campaign, Earth Syst. Sci. Data, 11, pp. 341–353, https://doi.org/10.5194/essd-11-341-2019.

[4] Westwater, E.R., (1978). The accuracy of water vapor and cloud liquid determination by dual-frequency ground based microwave radiometry, Radio Sci., 13, pp. 677–685, https://doi.org/10.1029/RS013i004p00677.

[5] Westwater, E.R., and Guiraud, F.O. (1980). Ground-based microwave radiometric retrieval of precipitable water vapor in presence of clouds with high liquid content, Radio Sci., 15, 947–957, https://doi.org/10.1029/RS015i005p00947.

[6] Crewell, S., and Loöhnert, U. (2003). Accuracy of cloud liquid water path from ground-based microwave radiometry, 2,Sensor accuracy and synergy, Radio Sci., 38(3), 8042, https://doi.org/10.1029/2002RS002634.

[7] Berrisford, P., Dee, D., Poli, P., Brugge, R., Fielding, K., Fuentes, M., Kllberg, P., Kobayashi, S., Uppala, S., and Simmons, A. (2011). The ERA-interim Archive Version 2.0, ERA Report Series 1, ECMWF, Shinfield Park, Reading, https://www.ecmwf.int/en/elibrary/8174-era-interim-archive-version-20.

[8] Dow, J.M., Neilan, R. E., and Rizos, C. (2009). The International GNSS Service in a changing landscape of Global Navigation Satellite Systems, J. Geod., 83, pp. 191–198, https://doi.org/10.1007/s00190-008-0300-3

[9] Eriksson, P., Buehler, S. A., Davis, C. P., Emde, C., and Lemke, O. (2011). ARTS, the atmospheric radiative transfer simulator, Version 2, J. Quant. Spectrosc. Radiat. Transfer, https://doi.org/10.1016/j.jqsrt.2011.03.001.

[10] Chen, P., Yao, W., and Zhu, X. (2014), Realization of global empirical model for mapping zenith wet delays onto precipitable water using NCEP re-analysis data, Geophys. J. Int., 198(3), pp. 1748–1757, https://doi.org/10.1093/gji/ggu223.

[11] Cimini, D., Rosenkranz, P.W., Tretyakov, M.Y., Koshelev, M.A. and Romano, F. (2018). Uncertainty of atmospheric microwave absorption model: impact on ground-based radiometer simulations and retrievals, Atmos. Chem. Phys., 18(20), pp. 15231–15259, https://doi.org/10.5194/acp-18-15231-2018.